The 2025 World Congress on
Advances in Structural Engineering and Mechanics (ASEM25)
BEXCO, Busan, Korea, August 11-14, 2025

Optimal Evacuation Route Analysis Considering Congestion During Disaster for the Underground station

Mintaek Yoo[1], Hyunseok Kim[2], *Changwon Kwak[3] and *Seongwon Hong[4]

[1), 2)] *Departemnt of Civil and Environmental Engineering, Gachon Univeristy 1342, Seongnam-daero, Sujeong-gu, Seongnam-si, Gyeonggi-do, Republic of Korea*
[3)] *Department of Civil and Environmental Engineering, Inha Technical College, 100, Inha-ro, Incheon, Korea*
[4)] *Department of Safety Engineering, Korea National University of Transportation, 50 Daehak-ro, Chungju-si, ChungBuk 27469, Republic of Korea*

[1)] *mintaekyoo@gachon.ac.kr*
[2)] *khsss1026@gachon.ac.kr*
[3)] *geotech@gachon.ac.kr*
[4)] *shong@ut.ac.kr*

ABSTRACT

Evacuation efficiency in deep underground stations is highly sensitive to disaster-induced congestion and dynamic pedestrian behavior. This study introduces a real-time evacuation simulation framework that evaluates and adapts optimal paths based on the progression of fire and the spatial distribution of evacuees. Instead of relying on fixed assumptions, this model integrates congestion-sensitive travel time recalculation into the pathfinding process. A virtual six-level underground station is constructed as a node-edge graph, and three fire scenarios are implemented by altering node accessibility. The simulation demonstrates that blockage at highly congested zones causes significantly longer evacuation durations, highlighting the importance of hazard-aware path reallocation in underground station design.

1. INTRODUCTION

In recent decades, the concentration of urban populations has prompted the extensive development of subsurface infrastructure, such as metro systems, underground shopping complexes, and deep-level transit facilities. These underground environments play an increasingly vital role in modern cities, but they also present unique risks during emergencies. Restricted visibility, complex layouts, dense occupancy, and

---

[1)] Professor
[2)] Undergraduate student
[3)] Professor, corresponding author
[4)] Professor, corresponding author

limited points of egress contribute to their vulnerability. For example, the catastrophic subway fire that occurred in Daegu, South Korea, in 2003 resulted in 198 fatalities and 146 injuries (Yuan et al., 2022). More recently, unprecedented rainfall in Seoul during 2022 led to the flooding of multiple underground stations, causing seven deaths and significant service disruptions (Cao et al., 2024). These incidents highlight the critical necessity for effective emergency evacuation strategies in subterranean facilities.

When crowd levels are high, particularly during peak operating hours, the movement of evacuees can become severely restricted due to congestion, resulting in slower overall evacuation rates (Kim and Chung, 2019). Although considerable research has examined the structural performance and seismic resistance of underground facilities (Liu et al., 2018; Yang et al., 2020; Kwon et al., 2020), far fewer studies have addressed the operational safety of occupants during emergencies. The absence of reliable evacuation models that account for dynamic crowding effects and evolving hazard conditions leaves a major gap in current disaster planning frameworks.

To address this, a growing number of researchers have explored human-centric risk models. For instance, Yao et al. (2022) found that smoke-induced visibility reduction exerts a greater impact on evacuation effectiveness than elevated temperatures or toxic gas concentrations. Similarly, Wu et al. (2018) used Bayesian network approaches to evaluate fire risk in complex transit facilities, while Wang et al. (2021) developed spatial zoning models that incorporate occupant loads and exit widths to estimate evacuation risk in underground malls. Other works, such as Jin et al. (2020) and Xu et al. (2020), emphasize the critical influence of spatial layout and pedestrian congestion on evacuation outcomes.

From a computational perspective, the Dijkstra algorithm is widely used for determining optimal paths in network-based systems. Prior studies have utilized Dijkstra-based methods to simulate building evacuations under fire conditions (Zhang et al., 2021; Mirahadi et al., 2021), often integrating real-time hazard progression and environmental feedback into the routing process. Nevertheless, most of these models have either assumed static crowding conditions or lacked realistic updates in pedestrian travel speeds as congestion changes.

In response to this research gap, the present study proposes a dynamic evacuation modeling approach for deep underground stations using Dijkstra's algorithm. The model continuously adjusts pedestrian travel time in response to crowd density at each time step. To assess its performance, a six-level subway station was modeled as a node-edge graph, and three distinct fire scenarios were simulated by altering node accessibility. The goal is to evaluate whether this framework can minimize evacuation delays and improve resilience in emergency situations.

2. RESEARCH METHOLOGY

2.1 Dijkstra Algorithm

Dijkstra's algorithm is a representative method for optimal pathfinding. It determines the minimum cost between a start and end node on a graph consisting of nodes and edges, and identifies the optimal evacuation route accordingly. The operation of Dijkstra's algorithm proceeds as follows: a graph is defined by specifying nodes and edges, the

start node is set, and the end node is designated as the fixed destination. The initial cost of the start node is set to zero, while all other nodes are assigned an infinite value. The algorithm then iteratively updates the costs starting from the nodes adjacent to the start node. (Rachmawati and Gustin, 2020) For example, assuming the start node is io and a neighboring node is ix, the algorithm compares the sum of the edges weight between io and ix and the cost of io, with the current cost of ix. Since the initial cost of io is 0 and that of ix is infinity, the algorithm compares 0 + edge (io, ix) with infinity. ix is then updated to the smaller of the two values. As its initial value is infinity, the update always occurs in the first iteration. This computation follows a blind search approach, exploring all possible paths and comparing their total weights to determine the optimal route with the minimum cost. In other words, since it explores all possible paths within the solution space, it is theoretically guaranteed to find the optimal route. (Amr et al., 2022) However, as Dijkstra's algorithm examines all potential paths, it incurs high computational cost. As the complexity of the solution space or the number of nodes increases, the computational load grows accordingly. Despite its computational cost, Dijkstra's algorithm was adopted in this study, as the primary focus was on obtaining an accurate solution rather than minimizing computation time. This choice was made to ensure the reliability and accuracy of the analysis results. Despite the longer computation time, identifying an accurate evacuation route aligns more closely with the objective of this study. The computational procedure of Dijkstra's algorithm is illustrated in Fig. 1.

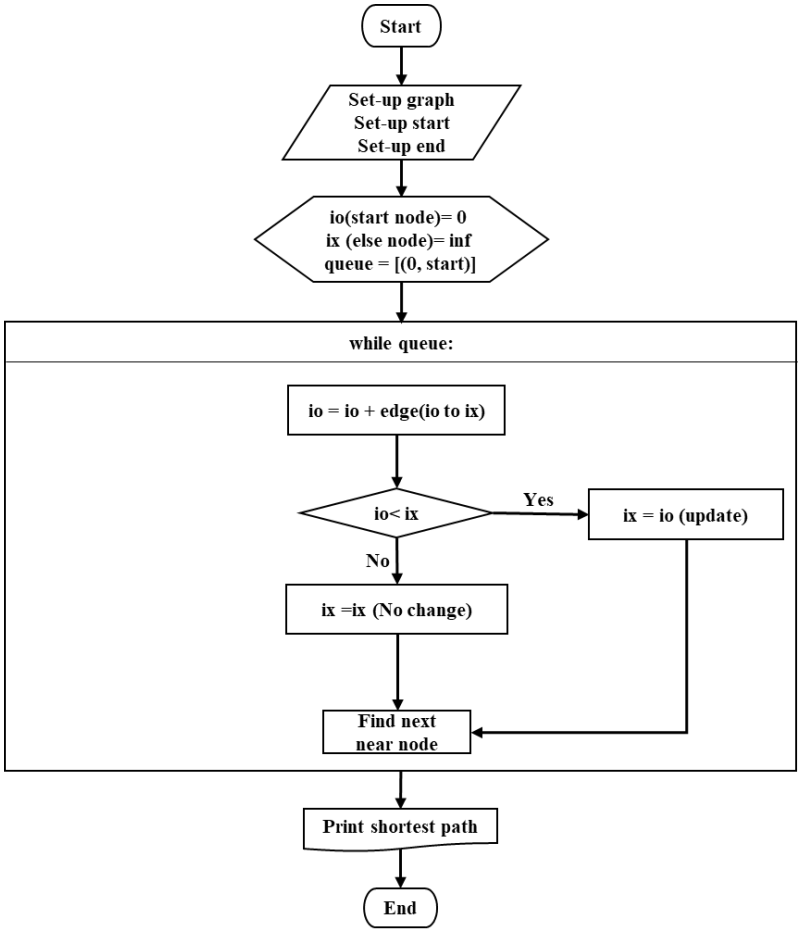

Fig 1. Dijkstra Algorithm Process

2.2 Process for deriving optimal evacuation route

In this study, an optimal evacuation route model based on Dijkstra's algorithm was developed to determine the best evacuation paths under varying levels of crowd density. Python was used to implement the model, and a total of four functions were developed. The functions used in the optimal evacuation route model based on crowd density are described as follows.

Function_1 implements the Dijkstra algorithm and calculates the optimal path as described in Section 2.1. After determining the optimal path, it identifies the next node in each evacuee's movement sequence. function_2 accumulates the evacuation route by repeatedly calling function_1 to construct the complete route. Once the end node is reached, it backtracks from the destination to identify the optimal

Fig 2. Process for deriving optimal evacuation route

evacuation route corresponding to the minimum cumulative cost. function_3 updates edge weights in real time based on evacuee movement information. This function is executed every second and adjusts edge values according to predefined congestion-related conditions. When crowd density increases, the edge weights are updated accordingly; when the density decreases, the updates are released. function_4 updates the movement information of evacuees. It consists of three components: transit_state, which stores information on evacuees currently in transit; current_count, which tracks evacuees who have arrived at each node; and travel_time, which records travel time data for each movement.

The function operates as follows: initially, the evacuees are assigned to current_count. Using function_1, the next optimal node is computed via the Dijkstra algorithm. Based on this result, the start node, end node, number of evacuees in transit, and their corresponding travel_time are recorded in transit_state. Using the information in transit_state, function_3 updates the edge weights to reflect the current movement of evacuees. For example, if transit_state contains the following information — start node: 0, end node: 12, travel_time: 10, and people_count: 100 — it indicates that 100 evacuees are currently moving from node 0 to node 12, with a travel time of 10 seconds. During the simulation, if multiple entries in transit_state share the same start node and end node, the evacuee counts are aggregated. Based on the total number of evacuees, a predefined congestion-based speed reduction factor is applied to update the corresponding edge weight. The simulation proceeds in one-second intervals, during which edge weights are updated and the travel_time values are reduced by one at each step. When travel_time reaches zero, the evacuees are considered to have arrived at the end node and are reassigned to current_count.

This process is iteratively repeated to simulate the evacuation. The simulation ends when all evacuees have successfully reached their destinations. A schematic representation of this process is shown in Fig. 2.

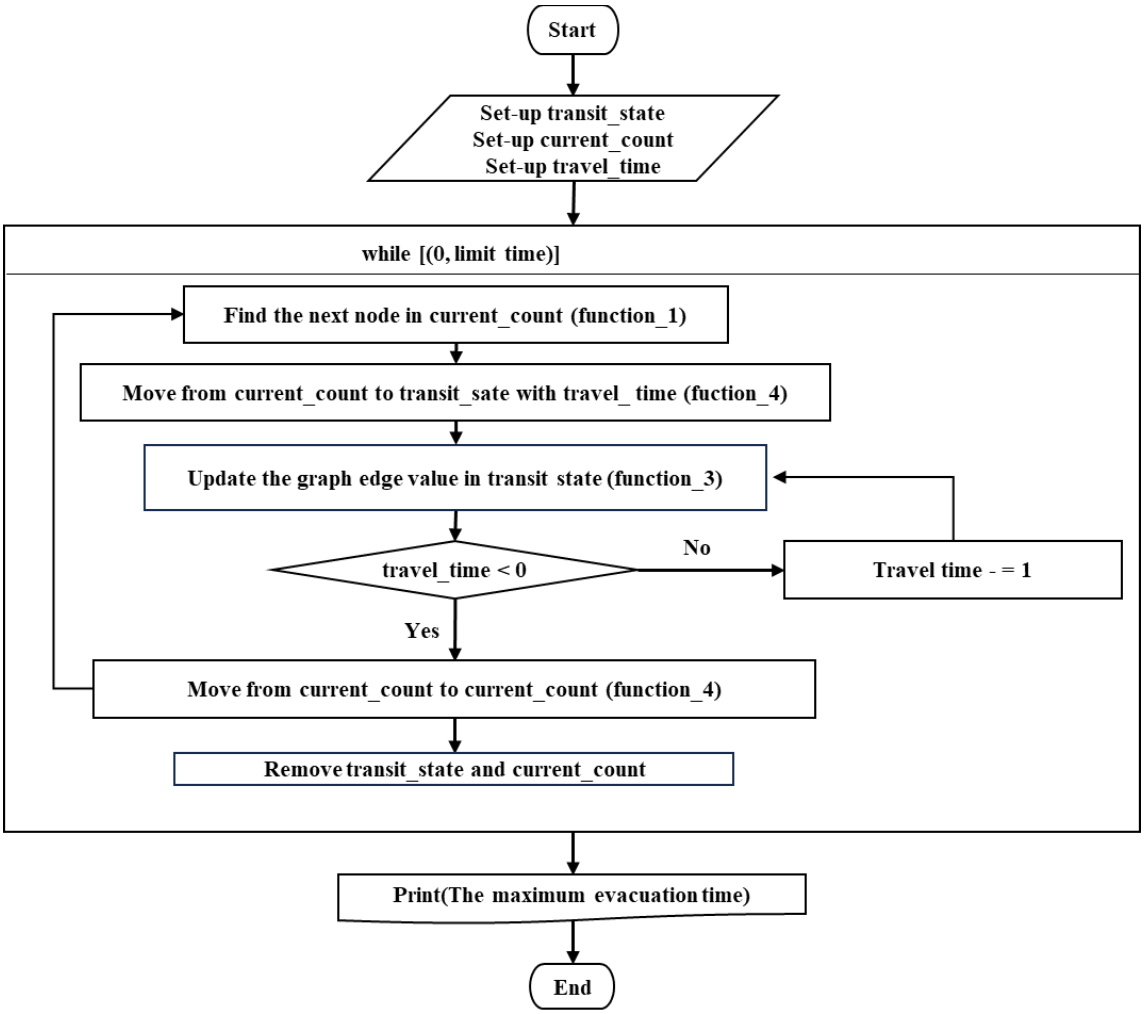

Fig 2. Process for deriving optimal evacuation route

3. ANALYSIS CONDITION

3.1 Modeling of underground structure

In order to realistically simulate evacuation dynamics in disaster situations, a detailed structural model of a deep underground subway station was developed. The modeled station was based on a representative six-level underground facility located in Seoul, South Korea. The geometry and layout of the station were constructed to reflect common characteristics of modern urban subway infrastructure.

The B6 level, where subway trains typically arrive and depart, was assumed to include platforms capable of accommodating 8-car trains, corresponding to an approximate length of 150 meters and a width of 50 meters. To discretize the structure, nodes were assigned at 50-meter intervals along the horizontal direction, allowing for sufficient resolution in representing lateral movement.

In the vertical direction, inter-floor connections were modeled using stairways with a slope of 45 degrees. With a vertical height of 5 meters between floors, this configuration results in an effective travel path length of approximately 7 meters between adjacent

levels. Edges connecting nodes were defined only where physical connections exist in the actual station layout. This selective edge assignment ensured that the simulation reflects realistic movement constraints by preventing transitions between unrelated areas. The final station model consisted of 70 nodes spanning six basement levels and included both horizontal and vertical movement pathways. This model served as the basis for the dynamic simulation of evacuation under various congestion and disaster scenarios. The complete node configuration is illustrated in Fig. 3.

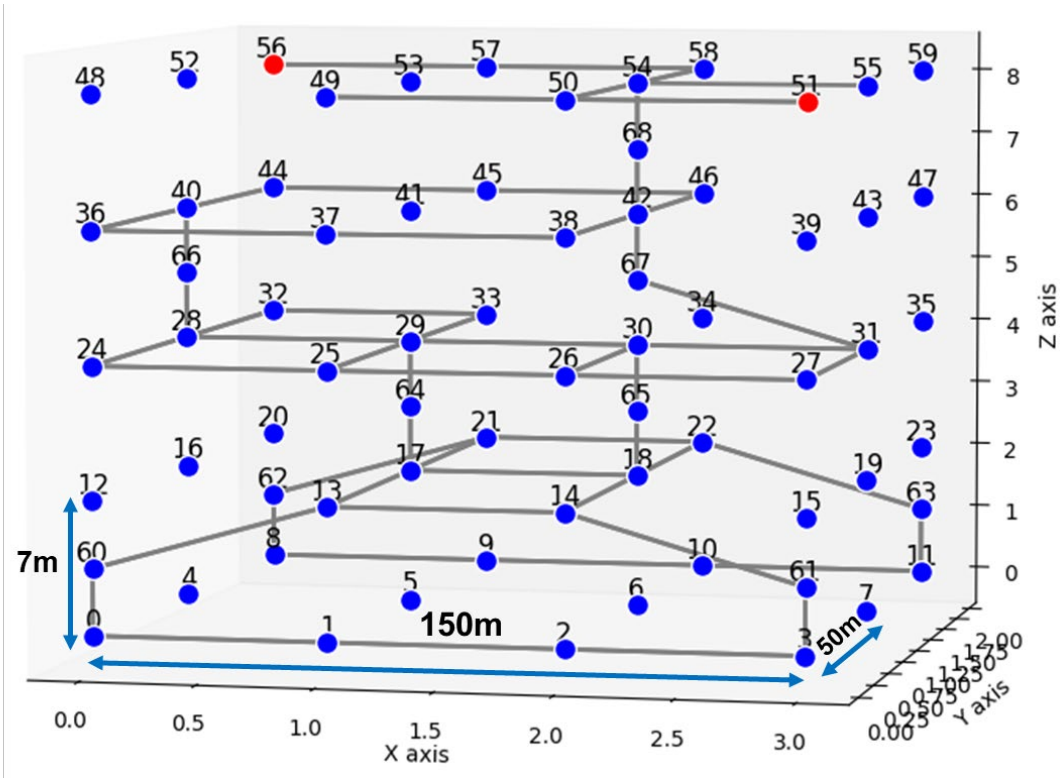

Fig 3. Node-based modeling of the deep underground station structure

3.2 Evacuation modeling parameter

To simulate evacuation behavior under realistic conditions, the initial distribution of evacuees was defined based on assumed occupancy patterns within the station. The B6 platform level, where train arrival and departure occur, was considered the most densely populated. Specifically, it was assumed that 2,000 evacuees were located on the train-side platform and 600 on the opposite platform, reflecting peak-hour passenger volumes typically observed in metropolitan subway systems during morning and evening rush hours. These assumptions are aligned with passenger flow data reported by the Seoul Metro Authority for high-density transfer stations.

In addition to the B6 level, each of the upper floors was assigned a smaller number of evacuees to represent individuals transiting within the station for transfer or access to commercial areas. The number of evacuees on these floors ranged from 100 to 300 per level, resulting in a total of 3,200 individuals within the station at the start of the simulation. This distribution reflects both boarding passengers and transient occupants and was

designed to emulate typical operational conditions of a six-level deep underground station. The floor-by-floor population distribution is summarized in Table 1.

Table 1. Population distribution by underground floor

B6	B5	B4	B3	B2	B1	Total (person)
2600*	100	-	100	100	300	3200

*Train platform: 2,000; Opposite platform: 600

To parameterize pedestrian movement, the baseline walking speed was set at 60 meters per minute for horizontal movement and 15 meters per minute for vertical movement, as recommended by the Korean Ministry of Land, Infrastructure and Transport's "Design Guidelines for Urban Railway Stations and Transfer Facilities." These values represent average mobility under uncongested public transit conditions.

Congestion effects were incorporated to account for reduced movement efficiency at higher occupant densities. According to national standards, the maximum evacuation capacity is 80 persons per meter per minute for horizontal flow and 60 persons per meter per minute for vertical flow. Considering typical dimensions—8 meters for platforms and 6 meters for stairs—the model defined critical thresholds of 640 and 360 individuals, respectively. When the number of evacuees exceeded these values, a congestion-induced slowdown was applied. Specifically, a tiered multiplier system was introduced: speeds were reduced by factors of 2.0, 2.5, or 3.0 depending on congestion levels, as summarized in Table 2. These multipliers were reflected in the edge weights of the node-edge graph to dynamically update travel times.

This adaptive mechanism played a crucial role in capturing nonlinear evacuation dynamics, such as bottleneck formation, feedback congestion, and time-dependent delays. It also ensured that evacuees continuously reassessed their routes as real-time congestion evolved, enhancing the realism and responsiveness of the simulation under disaster conditions.

Table 2. Congestion-based movement speed reduction factors

Evacuation Factor	Population (person)	Multiplier
Horizontal transportation	640	2
	1,280	2.5
	1,920	3
Vertical transportation	360	2
	720	2.5
	1080	3

3.3 Disaster condition by fire

To evaluate the impact of fire disasters on evacuation performance, three representative fire scenarios were defined based on their potential to disrupt evacuation flow. In each scenario, the affected node was treated as an impassable area by reducing the movement speed along the corresponding edge to 1% of its normal value. This approach effectively forces evacuees to avoid routes passing through the disaster location, thereby allowing the model to simulate rerouting behavior under emergency conditions.
Case 1 assumes a fire outbreak on the B6 platform where the train is arriving, specifically at node 0. This scenario reflects a critical situation where the most heavily populated area at the beginning of the evacuation becomes inaccessible due to a fire onboard or near the platform. Case 2 considers a fire at node 30, which was identified as the most congested node during the baseline evacuation scenario without any disaster. This represents a worst-case scenario where the blockage of a highly trafficked area could significantly increase rerouting congestion and overall evacuation time. Case 3 involves a fire at node 29, which showed moderate congestion in the baseline case. Although not as critical as node 30, its disruption is expected to have a non-negligible impact on the evacuation process due to its connectivity within the overall station layout. The definition and location of each disaster scenario are summarized in Table 3, and the spatial distribution of the disaster nodes is illustrated in Figure 4.
These scenarios were selected to assess how different types of disruption—whether at the origin of congestion, a critical node, or a moderately important connection—affect evacuation dynamics, maximum travel times, and congestion patterns throughout the network.

Table 3. Disaster scenario definition

Case No.	Scenario	Disaster node
Case 1	Fire at the train platform	0
Case 2	Fire at the most congested node	30
Case 3	Fire at moderately congested node	29

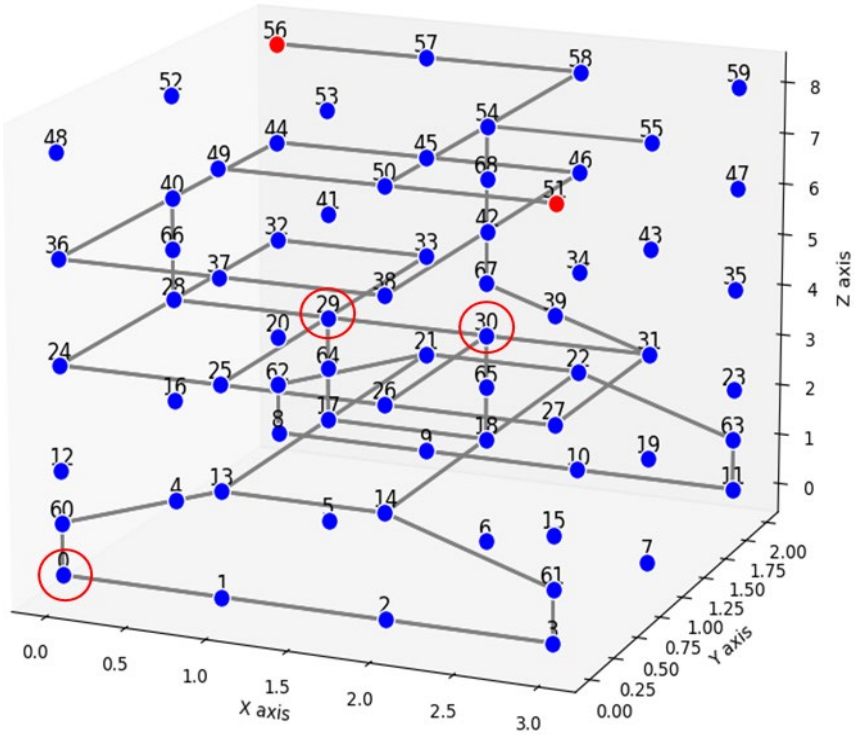

Fig 4. Spatial distribution of disaster nodes for each scenario

4. ANALYSIS RESULTS

The simulation results for each disaster scenario were analyzed in terms of maximum evacuation time, which represents the time required for the last evacuee to reach a safe location. The outcomes are summarized in Table 4.

Table 4. Summary of maximum evacuation time by disaster scenario

Case No.	Scenario	Maximum Evacuation Time (s)
Case 0	No disaster (baseline)	476
Case 1	Fire at the train platform (node 0)	490
Case 2	Fire at the most congested node (node 30)	704
Case 3	Fire at moderately congested node (node 29)	534

As shown in Table 4, all disaster scenarios resulted in increased maximum evacuation times compared to the baseline (Case 0). In Case 1, where a fire occurred at the B6 train platform (node 0), the maximum evacuation time increased by 14 seconds (from 476 to 490 seconds). This minor delay is attributed to localized rerouting of evacuees from the primary egress path, causing temporary congestion on secondary routes. In Case 2, which involved a fire at the most congested node (node 30), the evacuation time rose sharply to 704 seconds, representing a 228-second increase over the baseline. This indicates that the failure of a critical junction leads to substantial congestion and severely

disrupts evacuation efficiency across the network. In Case 3, where the fire occurred at a moderately congested node (node 29), the maximum evacuation time was 534 seconds, reflecting a 58-second increase compared to the baseline. Although the impact was less severe than in Case 2, it still demonstrates that disruptions at even moderately important nodes can noticeably hinder evacuation performance.

To analyze route changes under different fire scenarios, evacuation paths from Node 1—identified as one of the departure nodes with the longest evacuation time—were extracted and compared across scenarios. Specifically, the route under the no-disaster condition (Case 0) was used as a baseline for comparison. In Case 1 (fire at the train platform, Node 0), the original path 1-0-60-13-17-64-29-30 was rerouted to 1-2-3-61-14-48-65-30, indicating a shift away from the affected platform area. In Case 2, where the fire occurred at the most congested node (Node 30), the original path through 29-30-31-67 was rerouted to 29-25-26-27-31-67, avoiding the critical junction at Node 30.

In Case 3, with the fire at a moderately congested node (Node 29), the original path 13-17-64-29-30 was altered to 13-14-18-65-30, bypassing the disrupted node.These route changes under each disaster scenario are visualized with red lines in Fig. 5, and detailed evacuation paths are summarized in Table 5.

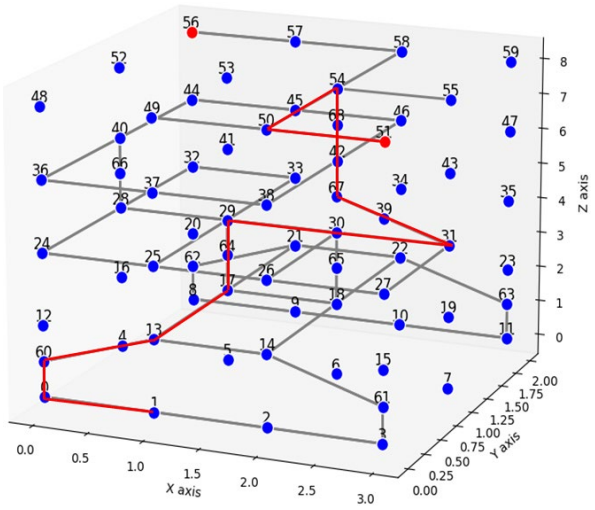

Case 0

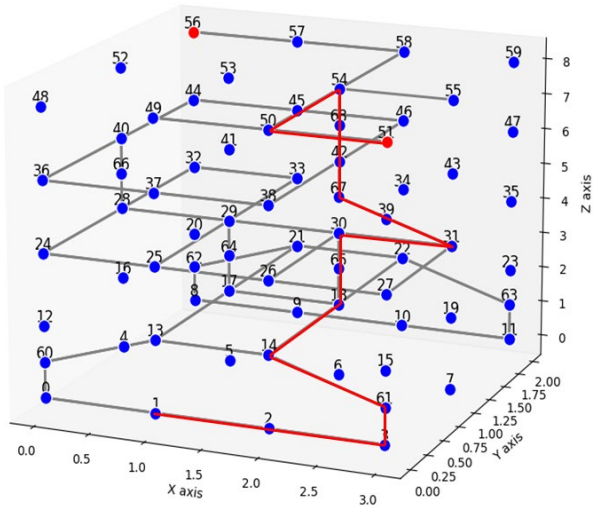

Case 1

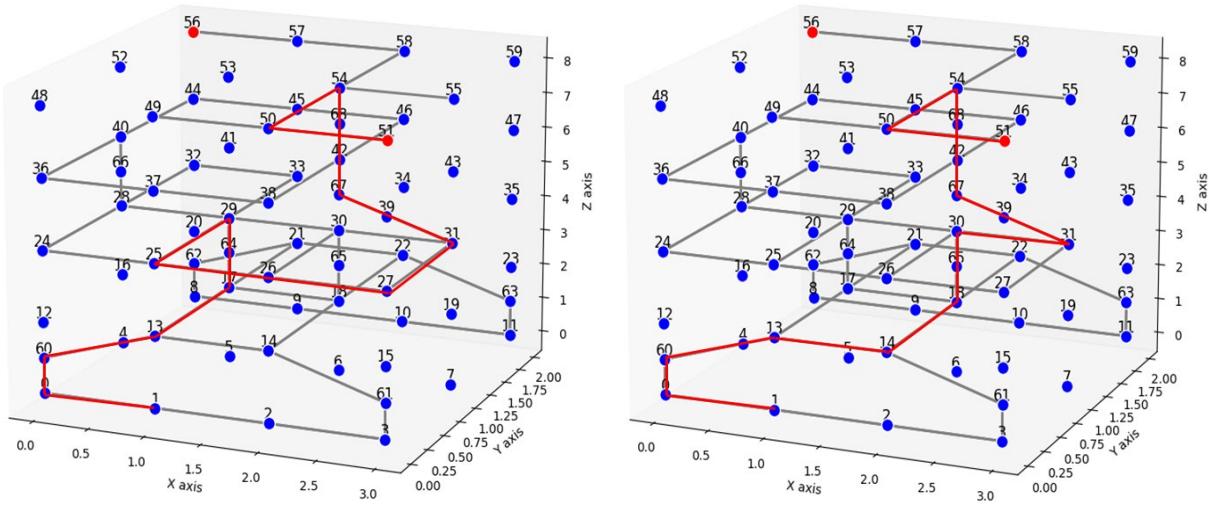

Case 2 Case 3

Fig 5. Evacuation route changes from Start Node 1

Table 5. Case-by-case route changes from Start Node 1

Case No.	Evacuation Route																
Case 0	1	0	60	13	17	64	29	30	31	67	42	68	54	50	51		
Case 1	1	0	60	13	17	64	29	25	26	27	31	67	42	68	54	50	51
Case 2	1	0	60	13	14	18	65	30	31	67	42	68	54	50	51		
Case 3	1	2	3	61	14	18	65	30	31	67	42	68	54	50	51		

These results highlight the importance of congestion-aware evacuation modeling and scenario-based risk evaluation in deep underground station designs. In particular, they underscore the need to identify and protect high-impact nodes that act as bottlenecks in the evacuation network.

5. CONCLUSION

This study developed a congestion-aware evacuation simulation model for deep underground station environments using Dijkstra's algorithm. The following key conclusions were drawn based on the simulation results and scenario-based analysis:

1. The application of Dijkstra's algorithm enabled optimal path identification under dynamic conditions by continuously updating edge weights based on real-time congestion levels. This approach ensured accurate representation of evacuee movement and decision-making during emergencies.

2. Fire scenarios significantly influenced evacuation performance, with maximum evacuation time increasing when key nodes were blocked. In particular, the

scenario involving a fire at the most congested node (Case 2) resulted in the largest delay, confirming the critical role of node centrality and connectivity in evacuation efficiency.

3. Even moderate disruptions led to meaningful evacuation delays. The fire at a moderately congested node (Case 3) increased evacuation time by approximately 50 seconds, highlighting the need for scenario-based risk assessment even in non-critical areas.

4. The baseline (no-disaster) scenario produced the shortest evacuation time, serving as a reference for evaluating disruption impact. The contrast between baseline and disaster scenarios emphasizes the importance of maintaining accessibility to high-flow paths under emergency conditions.

5. The proposed model provides a practical framework for identifying evacuation vulnerabilities, quantifying the effects of congestion, and planning structural or operational interventions in underground station design. Future research should incorporate additional factors such as human behavior, smoke propagation, vertical circulation constraints, and multi-agent interactions to enhance realism and decision support capability in complex disaster scenarios.

REFERENCES

Yuan, Q., Zhu, H., Zhang, X., Zhang, B., Zhang, X. (2022), “An integrated quantitative risk assessment method for underground engineering fires,” Int. J. Environ. Res. Public Health, 19(24), 16934. https://doi.org/10.3390/ijerph192416934

Cao, S., Wang, M., Zeng, G., Li, X. (2024), “Simulation of crowd evacuation in subway stations under flood disasters,” IEEE Trans. Intell. Transp. Syst., 25(9), 11858–11867.

Kim, J., Chung, J. (2019), “Design proposal to help evacuate in case of subway fire,” J. Digit. Contents Soc., 20(9), 1727–1736.

Liu, N., Huang, Q.B., Fan, W., Ma, Y.J., Peng, J.B. (2018), “Seismic responses of a metro tunnel in a ground fissure site,” Geomech. Eng., 15(2), 775–781. https://doi.org/10.12989/gae.2018.15.2.775

Yang, S., Kwak, D., Kishida, T. (2020), “Development of seismic fragility curves for high-speed railway system using earthquake case histories,” Geomech. Eng., 21(2), 179–186. https://doi.org/10.12989/gae.2020.21.2.179

Kwon, S.Y., Yoo, M., Hong, S. (2020), “Earthquake risk assessment of underground railway station by fragility analysis based on numerical simulation,” Geomech. Eng., 21(2), 143–152. https://doi.org/10.12989/gae.2020.21.2.143

Yao, H.-W., Lv, K.-F., Li, Y.-X., Zhang, J.-G., Lv, Z.-B., Wang, D., Zhan, Z.-Y., Wei, X.-G., Song, H.-T., Qin, H.-J. (2022), “Numerical simulation of fire in underground commercial street,” Comput. Intell. Neurosci., Article ID 4699471.

Wu, J., Hu, Z., Chen, J., Li, Z. (2018), “Risk assessment of underground subway stations to fire disasters using Bayesian network,” Sustainability, 10(10), 3810.

Wang, N., Gao, Y., Li, C., Gai, W. (2021), “Integrated agent-based simulation and evacuation risk-assessment model for underground building fire: A case study,” J. Build. Eng., 40, 102609.

Jin, B., Wang, J., Wang, Y., Gu, Y., Wang, Z. (2020), “Temporal and spatial distribution of pedestrians in subway evacuation under node failure by multi-hazards,” Saf. Sci., 127, 104695. https://doi.org/10.1016/j.ssci.2020.104695

Xu, H., Tian, C., Li, Y. (2020), “Emergency evacuation simulation and optimization for a complex rail transit station: A perspective of promoting transportation safety,” J. Adv. Transp., Article ID 8791503.

Zhang, H., Zhao, Q., Cheng, Z., Liu, L., Su, Y. (2021), “Dynamic path optimization with real-time information for emergency evacuation,” Math. Probl. Eng., Article ID 3017607.

Mirahadi, F., McCabe, B.Y. (2021), “EvacuSafe: A real-time model for building evacuation based on Dijkstra’s algorithm,” J. Build. Eng., 34, 101687.

Rachmawati, D., Gustin, L. (2020), “Analysis of Dijkstra’s Algorithm and A Algorithm in Shortest Path Problem,” J. Phys. Conf. Ser., 1566, 012061.

Amr, M., Bahgat, A., Rashad, H., Ibrahim, A. (2022), “Comparison of Path Planning between Improved Informed and Uninformed Algorithms for Mobile Robot,” Int. J. Adv. Comput. Sci. Appl., 13(6), 239–248.

Ministry of Land, Infrastructure and Transport (2022), “Design Guidelines for Urban Railway Stations and Transfer Facilities,” Notice No. 2022-78, Sejong, Republic of Korea.